

Effect of dehydration of $\text{VOPO}_4 \cdot 2\text{H}_2\text{O}$ on the preparation and reactivity of vanadium phosphate catalyst for the oxidation of *n*-butane

F. Javier Cabello Sanchez, J. Antonio Lopez-Sanchez, Richard P.K. Wells, Colin Rhodes, Asghar-Zeini Isfahani* and Graham Hutchings**

Department of Chemistry, Cardiff University, PO Box 912, Cardiff CF10 3TB, UK
E-mail: hutch@cardiff.ac.uk

Received 5 June 2001; accepted 26 September 2001

The effect of drying of $\text{VOPO}_4 \cdot 2\text{H}_2\text{O}$ on the preparation of vanadium phosphate catalysts for the selective oxidation of *n*-butane to maleic anhydride is described and discussed. It is found that partially dehydrated samples of the dihydrate containing small amounts of α_1 - VOPO_4 are formed when the material is initially dried. The presence of this impurity leads to a final catalyst containing trace amounts of α_1 - VOPO_4 in combination with $(\text{VO})_2\text{P}_2\text{O}_7$ and this combination leads to a catalyst with a higher activity but with a lower selectivity to maleic anhydride. The drying stage is also found to influence the surface area and intrinsic activity of the activated catalyst.

KEY WORDS: vanadium phosphate preparation; *n*-butane oxidation; maleic anhydride

1. Introduction

There is at present considerable interest in the preparation of vanadium phosphate catalyst for the selective oxidation of *n*-butane to produce maleic anhydride [1–3]. At present, the preferred industrial catalysts are derived from *in situ* activation under reaction conditions of the catalyst precursor $\text{VOHPO}_4 \cdot 0.5\text{H}_2\text{O}$ [4]. The activated catalysts comprise $(\text{VO})_2\text{P}_2\text{O}_7$ in combination with α_{II} - and δ - VOPO_4 phases [5], and many researchers consider that a specific combination of V^{4+} and V^{5+} phases is necessary for the catalyst to exhibit high activity and selectivity to maleic anhydride [6,7]. To date, a large number of methods to prepare $\text{VOHPO}_4 \cdot 0.5\text{H}_2\text{O}$ have been studied since it is readily crystallised from solution containing $(\text{VO})^{2+}$ and H_3PO_4 in the presence of aqueous HCl [4], or organic reducing agents, typically alcohols [8]. For example, refluxing V_2O_5 with H_3PO_4 in isobutanol produces very pure samples of $\text{VOHPO}_4 \cdot 0.5\text{H}_2\text{O}$ [9]. Recently, we have shown that $\text{VOHPO}_4 \cdot 0.5\text{H}_2\text{O}$ can be prepared by the reaction of $\text{VOPO}_4 \cdot 2\text{H}_2\text{O}$ with alcohols [10], and furthermore that the structure of the alcohol controls the morphology of $\text{VOHPO}_4 \cdot 0.5\text{H}_2\text{O}$. The highest catalytic activities and highest surface areas were obtained using primary alcohols [10]. For this preparation method we have now investigated the effect of drying $\text{VOPO}_4 \cdot 2\text{H}_2\text{O}$ prior to the reduction step with the alcohol. In this paper we show that control of this procedure is necessary to obtain the best catalytic performance.

* Present address: Department of Chemistry, University of Esfahan, Esfahan 81744, Iran.

** To whom correspondence should be addressed.

2. Experimental

2.1. Catalyst preparation

2.1.1. $\text{VOPO}_4 \cdot 2\text{H}_2\text{O}$

V_2O_5 (11.8 g, Aldrich) was refluxed with H_3PO_4 (115 g, 85%, Aldrich) in water (300 ml) for 8 h. The yellow $\text{VOPO}_4 \cdot 2\text{H}_2\text{O}$ was recovered by hot filtration, washed with water and acetone and dried in air (110 °C, 16 h).

2.1.2. $\text{VOHPO}_4 \cdot 0.5\text{H}_2\text{O}$

$\text{VOPO}_4 \cdot 2\text{H}_2\text{O}$ (8 g) was refluxed with isobutanol (160 ml) for 21 h. The blue solid was recovered by hot filtration, washed with isobutanol (200 ml) and ethanol (250 ml), dried in air (110 °C, 2 h), refluxed in water (10 ml g⁻¹, to remove $\text{VO}(\text{H}_2\text{PO}_4)_2$ which is often present as an impurity), filtered hot, washed with water and dried in air (110 °C, 16 h) prior to use as a catalyst.

2.2. Catalyst testing and characterisation

The oxidation of *n*-butane was carried out with a microreactor using a standard volume of catalyst (0.7 ml). *n*-butane and air were fed to the reactor *via* calibrated mass flow controllers to give a feedstock composition of 1.8% *n*-butane in air. The products were fed *via* heated lines to an on-line gas chromatograph for product analysis. The reactor comprised a stainless steel tube with catalyst held in place by plugs of quartz wool. A thermocouple was located on the centre of the catalyst bed and temperature control was typically ± 1 °C. Carbon mass balances of $\geq 95\%$ were typically observed. $\text{VOHPO}_4 \cdot 0.5\text{H}_2\text{O}$ precursors were activated *in situ* (1.8% *n*-butane in air, 2500 h⁻¹) at 400 °C for 72 h.

A number of physical techniques were employed to characterise the catalyst microstructure. Powder X-ray diffraction (XRD) was performed using an Enraf Nonius FR 590 X-ray generator with a Cu K_{α} source fitted with an Inel CPS120 hemispherical detector. BET surface area measurements using nitrogen adsorption were carried out using a Micromeritics ASAP 2000 instrument. Raman spectra were obtained using a Renishaw Ramanscope spectrograph fitted with a green Ar^{+} laser ($\lambda = 514.532$ nm). Thermal gravimetric analysis (TGA) was performed using a Perkin–Elmer TGA7 thermogravimetric analyser.

3. Results and discussion

3.1. Catalyst precursor characterisation

Four samples of $VOPO_4 \cdot 2H_2O$ were prepared using the standard procedure and were allowed to stand open to the atmosphere for 0, 1, 10 and 26 h after being dried at $110^{\circ}C$ for 16 h. The powder XRD patterns for the four dihydrate samples are shown in figure 1. It is apparent that the signal to noise ratio of the diffraction pattern improves with increased exposure to air. The two main reflections at 11.7° and 23.9° 2θ , can be assigned to the (001) and (002) crystallographic planes of $VOPO_4 \cdot 2H_2O$ [11]. There is a broad reflection at *ca.* 22° 2θ which cannot be assigned to $VOPO_4 \cdot 2H_2O$, but three $VOPO_4$ phases (α_1 , δ and γ) exhibit their most intense reflections in this region [11,12]. The laser Raman spectra for the dihydrate samples are shown in figure 2. The dihydrate is highly sensitive to dehydration in the laser beam and so to minimise this effect, the Raman spectra were collected using 10 s accumulation with a low laser power (4 mW) to avoid dehydration of the sample due to localised heating. Significant changes are apparent in the Raman spectra. In the sample that has been exposed to air for 10 and 26 h, the bands with Raman shifts of 1038, 991, 954 and 540 cm^{-1} can all be assigned to $VOPO_4 \cdot 2H_2O$ [11]. The additional Raman bands at 579 and 928 cm^{-1} can be assigned to α_1 - $VOPO_4$ [11] and the weak band at $1010\text{--}1020\text{ cm}^{-1}$ may be assigned to γ - or δ - $VOPO_4$. However, it is worth noting that the small band at 1010 cm^{-1} has been previously reported as a Raman shift of the monohydrate, $VOPO_4 \cdot H_2O$ [13–16]. It is apparent that the drying stage of the preparation for the dihydrate also partially dehydrates it to form α_1 - $VOPO_4$. However, the partially dehydrated material rehydrates on standing in air for a few hours.

The four samples of dihydrate were refluxed in isobutanol for 12 h and the XRD patterns of the catalyst, designated VPD0, VPD1, VPD10 and VPD26, are shown in figure 3. The corresponding Raman spectra all show a band at 988 cm^{-1} which is the most intense band in the Raman spectra of $VOHPO_4 \cdot 0.5H_2O$. However, as the samples are prepared using isobutanol, only the most intense band is observed as the remainder of the spectra is obscured due to fluorescence. The reflections in the powder XRD patterns of all four samples can be assigned to poorly crystalline $VOHPO_4 \cdot 0.5H_2O$. As expected for preparation in

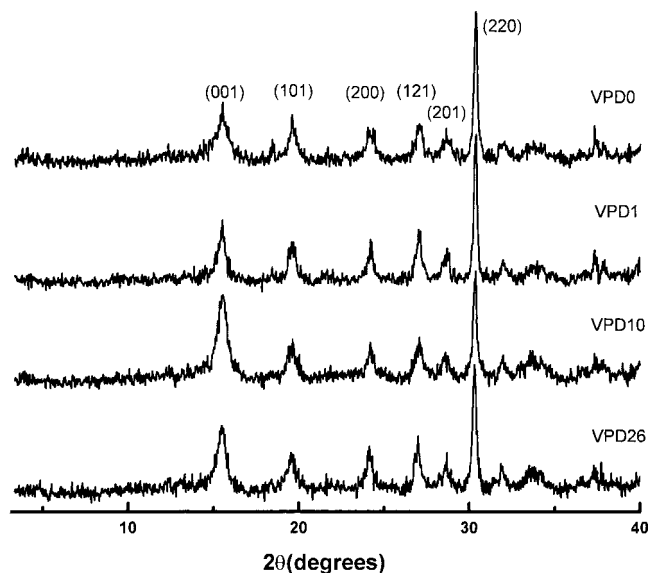


Figure 1. XRD patterns for the dihydrates.

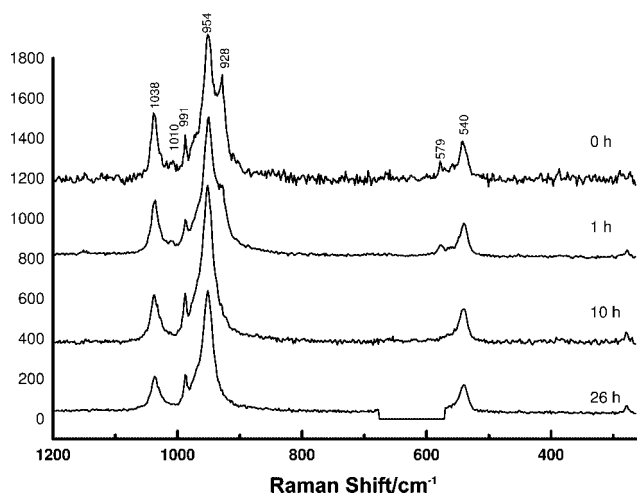


Figure 2. Raman spectra for the dihydrates.

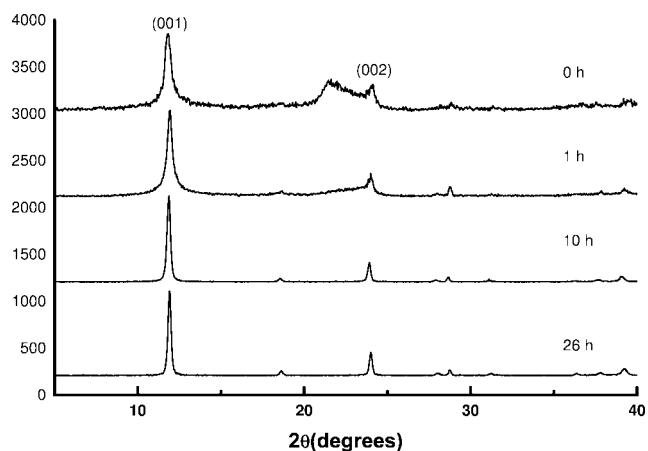


Figure 3. XRD patterns for the hemihydrates.

Table 1
n-butane oxidation over catalyst derived from $\text{VOHPO}_4 \cdot 0.5\text{H}_2\text{O}$.

Precursor	Surface area ($\text{m}^2 \text{g}^{-1}$)		<i>n</i> -butane conversion (%)	Selectivity (%)			Specific activity ($10^{-4} \text{ mol-MA g}^{-1} \text{ h}^{-1}$)	Intrinsic activity ($10^{-5} \text{ mol-MA m}^{-2} \text{ h}^{-1}$)
	Precursor	Activated catalyst		MA	CO	CO ₂		
VPD0	26	31	77	51	26	23	5.52	1.78
VPD1	19	29	74	47	27	26	4.93	1.70
VPD20	22	24	65	55	25	20	5.30	2.21
VPD26	18	22	65	58	23	19	5.30	2.39

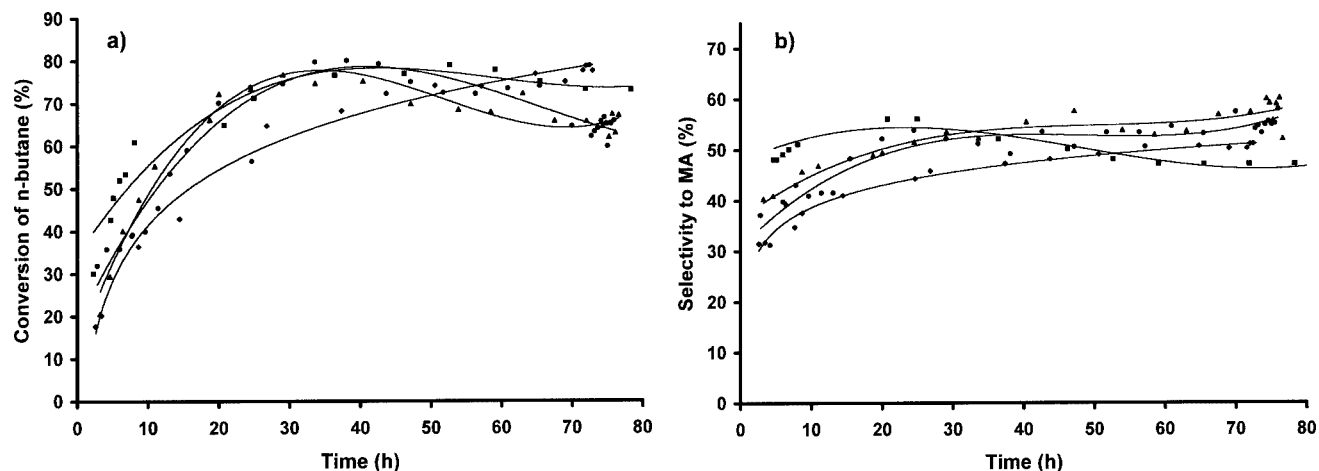


Figure 4. Catalyst performance for the conversion of *n*-butane: (a) conversion of *n*-butane and (b) maleic anhydride selectivity. (◆) VPD0, (■) VPD1, (●) VPD10 and (▲) VPD26.

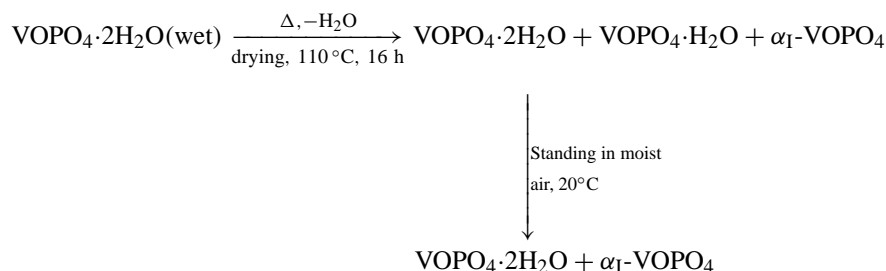
which $\text{VOPO}_4 \cdot 2\text{H}_2\text{O}$ is reduced with a primary alcohol [10] the most intense reflection is at $30^\circ 2\theta$ corresponding to the (220) plane of $\text{VOHPO}_4 \cdot 0.5\text{H}_2\text{O}$. The diffraction pattern was similar for all catalyst precursors. The only significant difference is that for the $\text{VOHPO}_4 \cdot 0.5\text{H}_2\text{O}$, the reflection for the (001) plane was slightly broader for VPD0, becoming relatively less broad and more intense for the VPD10 and VPD26 samples. The surface areas of the precursors were found to be highest for VPD0 (table 1). The TGA profiles of the $\text{VOHPO}_4 \cdot 0.5\text{H}_2\text{O}$ samples all showed two weight loss, at *ca.* 350 and 500 °C. The mass loss at *ca.* 350 °C was determined, using GCMS to be due to loss of isobutanol occluded within the hemihydrate crystals. The mass loss at 500 °C is considered to be due to the transformation of $\text{VOHPO}_4 \cdot 0.5\text{H}_2\text{O}$ to $(\text{VO})_2\text{P}_2\text{O}_7$ via dehydration [17]. The TGA profiles for VPD0, 1 and 10 were similar with the greatest mass loss at *ca.* 500 °C, and with VPD 26 the mass loss at *ca.* 350 °C being the largest feature.

3.2. *n*-butane oxidation studies and post-reaction characterisation

The four catalyst precursors were activated *in situ* using flowing *n*-butane (1.8%) in air at 400 °C for 72–75 h. During this time, the conversion of *n*-butane and the selectivity to maleic anhydride both increased and stabilised and the data are shown in figure 4 and table 1. The material prepared from VPD0 gives the highest conversion under these

conditions, and was still improving at the end of the catalyst test period. However, the VPD0 and VPD1 activated catalysts gave the lowest selectivity to maleic anhydride after the activation period of 80 h. On activation the surface area of all the materials is increased, with the most significant effect of VPD1. The specific activity ($\text{mol maleic anhydride g}^{-1} \text{ h}^{-1}$) for the four samples is very similar. However, the intrinsic activity ($\text{mol maleic anhydride m}^{-2} \text{ h}^{-1}$) clearly increases as the air exposure time for the dihydrate increases (table 1).

The catalyst structures were examined following reaction using powder XRD (figure 5) and laser Raman spectroscopy (figure 6). The XRD patterns of the four activated catalysts are very similar and the main reflections can all be assigned to poorly crystalline $(\text{VO})_2\text{P}_2\text{O}_7$. The only notable difference is that the reflection of the (200) plane decreases in intensity in the order $\text{VPD0} > \text{VPD1} > \text{VPD10} > \text{VPD26}$ (relative to the intensity of the most intense (024) reflection). The Raman spectra are also very similar and bands at 925(vs), 1130 and 1180 cm^{-1} can all be assigned to $(\text{VO})_2\text{P}_2\text{O}_7$ [11]. In addition, a weak band, which is particularly apparent with VPD0 and VPD1, is observed at 1038 cm^{-1} . This can be assigned to $\alpha_1\text{-VOPO}_4$ [11]. It is apparent, therefore, that the materials prepared with the dihydrate immediately following the drying stage (*e.g.*, 0 and 1 h) contain $\alpha_1\text{-VOPO}_4$ as well as the dihydrate. The activated catalysts derived from these precursors also contain $\alpha_1\text{-VOPO}_4$ and it is possible that this persists during the preparation. Previous studies by Abdelouahab *et al.* [16]



Scheme 1.

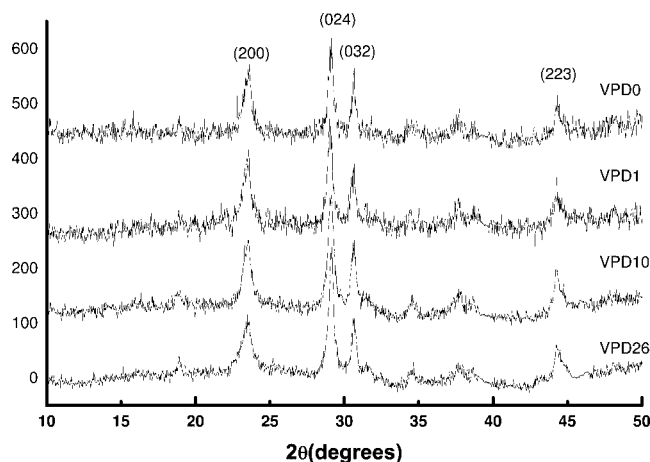


Figure 5. XRD patterns for the activated catalyst.

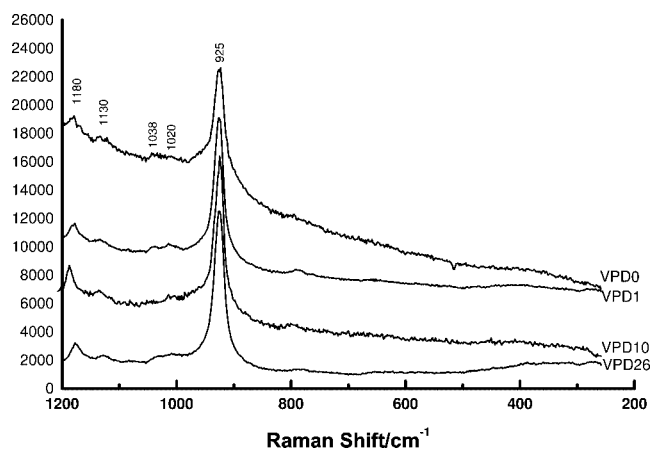


Figure 6. Raman spectra for the activated catalysts.

have shown that VOPO_4 phases are readily dehydrated, and a schematic representation of the processes occurring during the drying stage of the preparation of the dihydrate is shown in scheme 1.

It is proposed that the $\alpha_1\text{-VOPO}_4$ formed by the drying step remains unreacted with the isobutanol and is dispersed as a poorly crystalline material in the final activated cata-

lyst. $\alpha_1\text{-VOPO}_4$ is known to be less selective but more active than $(\text{VO})_2\text{P}_2\text{O}_7$ [1], and the combination of the two phases would be expected to produce a more active but less selective catalyst.

This study clearly shows that it is essential to control the drying step in the preparation of $\text{VOPO}_4 \cdot 2\text{H}_2\text{O}$. Furthermore, we show that this single preparation step can play a major role in controlling both the surface area and intrinsic activity of the recently activated catalyst prepared using this material.

References

- [1] G. Centi, *Forum on Vanadium Pyrophosphate Catalyst*, Catal. Today 16 (1994).
- [2] E. Bordes, Catal. Today 1 (1987) 499.
- [3] G.J. Hutchings, Appl. Catal. 72 (1992) 1.
- [4] G.J. Hutchings, A. Desmartin-Chomel, R. Olier and J.C. Volta, Nature 368 (1994) 41.
- [5] C.J. Kiely, A. Burrows, G.J. Hutchings, K.E. Bere, J.C. Volta, A. Tuel and M. Abon, Faraday Discuss. 105 (1996) 103.
- [6] G.W. Coulston, S.R. Bare, H. Kung, K. Birkeland, G.K. Bethke, R. Harlow, N. Herron and P.L. Lee, Science 275 (1997) 191.
- [7] J.T. Gleaves, J.R. Ebner and T.C. Kuechler, Catal. Rev. Sci. Eng. 30 (1988) 49.
- [8] G. Centi, Catal. Today 16 (1994) 1.
- [9] J.W. Johnson, D.C. Johnston, A.J. Jacobson and J.F. Brody, J. Am. Chem. Soc. 106 (1984) 8123.
- [10] M.T. Sananes, I.J. Ellison, S. Sajip, A. Burrows, C.J. Kiely, J.C. Volta and G.J. Hutchings, J. Chem. Soc. Faraday Trans. 92 (1996) 137.
- [11] F.B. Abdelouhab, R. Olier, N. Guilhaume, F. Lefebvre and J.C. Volta, J. Catal. 134 (1992) 157.
- [12] M.T. Sananes-Schulz, F.B. Abdelouhab, G.J. Hutchings and J.C. Volta, J. Catal. 163 (1996) 346.
- [13] M. Tachez, F. Theobald and E. Bordes, J. Solid State Chem. 40 (1981) 280.
- [14] C. R'kha, M.T. Vandendorre, J. Livage, R. Prost and E. Huard, J. Solid State Chem. 63 (1986) 202.
- [15] M. Tachez, F. Theobald, J. Bernard and A.W. Hewat, Rev. Chim. Miner. 19 (1982) 291.
- [16] F.B. Abdelouhab, J.C. Volta and R. Oliver, J. Catal. 148 (1994) 334.
- [17] V. Martin, J.M.M. Millet and J.C. Volta, J. Thermal Anal. 53 (1998) 111.